Measurement of the Rb D2 transition linewidth at ultralow temperature

B.E. Schultz, H. Ming, G.A. Noble, and W.A. van Wijngaarden[a]

Physics Dept., Petrie Bldg., York University, 4700 Keele St., Toronto, ON Canada, M3J 1P3, Canada

Abstract. The Rb D2 linewidth was studied using atoms cooled to a temperature of 50 μK that were contained in a magneto-optical trap. The transmission of a probe laser through the atom cloud was monitored using a CCD detector. The frequency of the probe laser was scanned across the resonance using an acousto-optic modulator. The observed lineshape was very well fitted by a Lorentzian function. The full width half maximum linewidth was examined as a function of the optical depth and the probe laser intensity. The extrapolated value at zero optical depth 6.062 ± 0.017 MHz corresponds to a $5P_{3/2}$ lifetime of 26.25 ± 0.07 ns. This result agrees with lifetimes found in experiments that measured the temporal decay of fluorescence or photoassociation spectroscopy and is somewhat below the result of a relativistic many body perturbation calculation.

PACS. 32.70.Jz Line shapes, widths, and shifts – 32.70.Cs Oscillator strengths, lifetimes, transition moments

1 Introduction

The development of laser cooling techniques [1] permits the production of atoms at temperatures where Doppler broadening is negligible. Excitation at optical wavelengths in ultracold atoms therefore allows the study of mechanisms that broaden the linewidth such as collisions as well as the natural transition linewidth itself [2,3]. The full width at half maximum (FWHM) linewidth γ is given by [4]

$$\gamma = \gamma_o \sqrt{1 + \frac{I}{I_s}} \tag{1}$$

where I is the light intensity, I_s is the saturation intensity for the transition and the natural linewidth is related to the excited state lifetime τ by

$$\gamma_o = \frac{1}{2\pi\tau}. \tag{2}$$

Nearly all lifetimes are derived from experiments that measure the temporal decay of fluorescence. Unfortunately, various groups have at times obtained conflicting results. For example, in the alkali atoms there have been disagreements at the 1% level between different experiments even though individual experiments report much smaller uncertainties, as well as discrepancies between experiment and theory [5]. In the case of sodium, this discrepancy was resolved by an experiment that measured

ᵃ e-mail: `wlaser@yorku.ca`

the natural linewidth of the $3S_{1/2} \rightarrow 3P_{3/2}$ transition using laser cooled atoms [2]. That experiment detected the fluorescence generated by a laser whose frequency was precisely scanned across the transition.

This experiment shows how the natural linewidth can be determined by studying the transmission of a laser beam through a cloud of ultracold atoms. The technique was tested by studying the ^{87}Rb $5S_{1/2} \rightarrow 5P_{3/2}$ transition. The $5P_{3/2}$ radiative lifetime corresponding to the measured natural linewidth was then compared to results of a number of independent experiments that have yielded consistent results for the $5P_{3/2}$ state lifetime [6–10] and with theory [11,12].

The laser intensity I transmitted through an atom cloud is given by

$$I = I_o e^{-N_c \sigma} \tag{3}$$

where I_o is the incident laser intensity, N_c is the column density and σ is the absorption cross section. For atoms cooled to ultralow temperatures where Doppler broadening is negligible, the absorption cross section is given by

$$\sigma = \frac{\sigma_o}{1 + \left(\frac{\nu - \nu_o}{\gamma/2}\right)^2} \tag{4}$$

where σ_o is the cross section at the resonance transition frequency ν_o and ν is the laser frequency. Hence, for an atom cloud having an optical depth,

$$\text{OD} = N_c \sigma_o \tag{5}$$

the natural linewidth can be determined by measuring the transmission of the laser as a function of the frequency ν. For small values of OD, the frequency dependence of the laser beam transmitted through the atom cloud is well approximated by a Lorentzian function.

This paper is organized as follows. First, the apparatus and procedure are described. Next, the results are discussed and corrections to the linewidth are examined. Finally, the natural linewidth is used to compute the radiative lifetime of the $5P_{3/2}$ state which is compared to that found by experiments that monitor the temporal decay of fluorescence or photoassociation spectroscopy as well as theoretical calculations.

2 Apparatus and procedure

The apparatus used to generate and probe ultracold atoms is shown in Figure 1. The operation of this system has been described in detail elsewhere [13,14], and only a brief overview will be given here. ^{87}Rb atoms were first collected in a magneto-optical trap (MOT) operating at a pressure of $\sim 10^{-9}$ Torr. The atoms were cooled from several hundred degrees Celsius using standard laser cooling techniques [1]. A laser beam pushed the atoms into a second MOT housed in an ultrahigh vacuum (UHV) quartz cell operating at a pressure of $\sim 10^{-11}$ Torr. The MOT was loaded for five seconds at a transfer frequency of 10 Hz. The atom cloud was then compressed magnetically for 12 ms and further cooled for 4 ms using polarization gradient cooling to a temperature of approximately 50 μK. Lower temperatures were not necessary as the Voigt absorption lineshape very closely resembles the Lorentzian natural lineshape and has a FWHM width that is only 5 kHz larger than the natural linewidth of the transition.

The ultracold atom cloud was probed using a laser beam having a wavelength of 780 nm (New Focus Vortex 6013). The single mode probe laser frequency was locked to the ^{87}Rb $5S_{1/2}$ ($F = 2$) $\rightarrow$ $5P_{3/2}$ ($F = 1$–3) crossover peak, where F denotes the hyperfine level, using a saturation absorption spectroscopic signal. This signal used to lock the laser frequency, was obtained using two photodiodes, PD_1 and PD_2, as illustrated in Figure 1. PD_1 detected the transmission of a probe laser beam that passed through the cell. The second photodiode, PD_2, detected one of the two counterpropagating laser beams that intersected in a Rb vapour cell. This signal showed saturation peaks superimposed on a Doppler broadened background. The subtraction of the two photodiode signals yielded a Doppler free signal which facilitated locking the laser frequency. The probe laser beam then passed through an optical isolator that suppressed reflected laser feedback by in excess of 34 dB to avoid laser frequency instability.

The frequency of the probe laser beam was controlled by an acousto-optic modulator (AOM) (Intra Action ATM-1001A2). Approximately 70% of the light was shifted on each of two passes of the laser beam through the AOM. Double passing the laser through the AOM produced a frequency shifted beam whose spatial position was independent of the AOM modulation frequency and
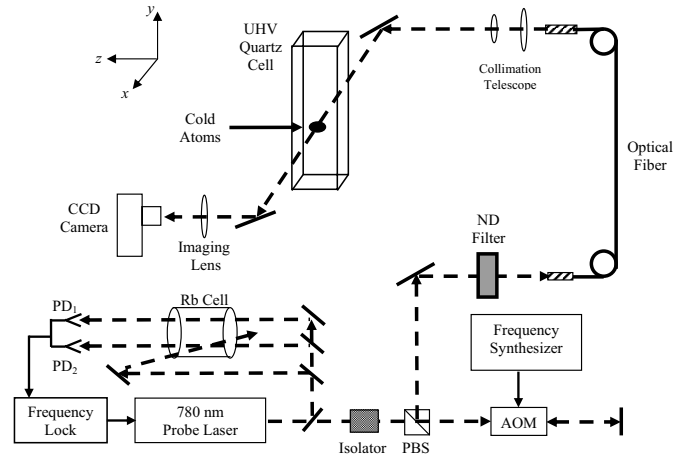

Fig. 1. Apparatus. The laser beam path is represented by the dashed line. See text for a detailed description.

thereby facilitated alignment of the laser with subsequent optical components. In our experiments, the AOM was used to increase the probe laser frequency by an amount ranging from 160 to 256 MHz, where a shift of 212 MHz corresponded to the ^{87}Rb $5S_{1/2}$ ($F = 2$) $\rightarrow$ $5P_{3/2}$ ($F = 3$) transition. The modulation frequency was monitored by a frequency meter (Optoelectronics 2810) with an accuracy of 1 kHz. The temporal duration of the probe laser pulse of 0.1 ms was controlled by adjusting the amplitude of the AOM modulation signal.

A polarizing beamsplitter (PBS) was used to input the laser into a single mode optical fiber that transported the laser beam to the UHV quartz cell housing the cold atoms. This ensured constant alignment of the laser beam relative to the ultracold atom cloud during the experiment. The laser beam exiting the fiber was collimated using a telescope, and directed through the UHV cell using mirrors. The probe laser beam incident on the atom cloud was linearly polarized in the vertical y direction and had a beam waist area of ≈ 0.5 cm^2. The laser power was varied using neutral density (ND) filters and measured using a power meter. The maximum available laser power was less than 100 μW. The laser beam transmitted through the atom cloud was imaged by a lens onto a CCD camera (Santa Barbara Model ST10XME) consisting of 2184×1472 pixels. Each pixel had an area of $(6.8~\mu\text{m})^2$. The CCD was mounted on a Peltier cooler which was turned on at least half an hour before images were recorded. The dark current was examined by taking an image with the laser blocked and found to be less than 1% of the signal strength. The size of the atom cloud as determined with the CCD was checked by measuring the gravitational acceleration of the atoms when released from the trap.

The UHV quartz cell was surrounded by three pairs of rectangular coils that cancelled the residual Earth's magnetic field to less than 10 mG as measured by a Hall effect gaussmeter. The MOT magnetic field as well as the cooling and repumper lasers were turned off 5 ms before the probe pulse to allow the decay of any induced currents
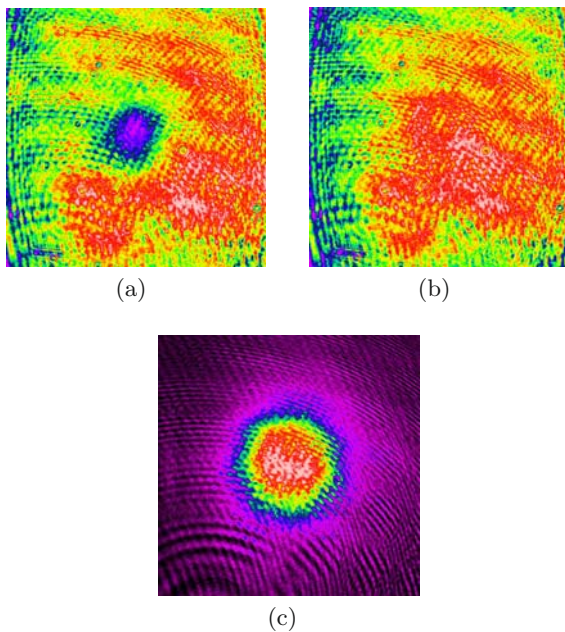
Fig. 2. (Color online) CCD images (1000×1000 pixels) showing probe laser beam absorption by ultracold atoms. CCD images of (a) laser absorption by atom cloud; (b) background with no atoms present; (c) result of background subtraction.

Fig. 3. Radial dependence of optical depth.

Fig. 4. (Color online) Sample Lorentzian fits of probe laser absorption to laser frequency. Data is shown for the central ring (black dots) and rings with radii 1.11 (red squares) and 2.24 (black triangles) mm. For convenience, the signal for the largest diameter ring is multiplied by a factor of 1.5. The data for each ring is fitted to a Lorentzian function.

in the MOT coils. A computer was interfaced to the current power supplies as well as to the AOM and CCD. A Labview 6.1 software program was written to control the timing of these instruments throughout the experiment.

The experimental procedure was as follows. Two separate CCD images were taken as shown in Figure 2 at each probe laser frequency. The first was an absorption image of the ultracold atom cloud, and the second was a background image taken with no atoms present. Figure 2c shows the atom cloud image resulting from the subtraction of the two images done by the CCD software [15]. The resulting image was fit to a Gaussian function to locate the atom cloud center. This image was then divided into 45 concentric rings where each ring had a width of 10 pixels. This encompassed the maximum unobstructed region that could be viewed as the quartz cell was surrounded by the MOT coils. For each ring, the average absorption of the probe laser or optical depth was found and plotted as a function of the radius as shown in Figure 3. The optical depth is maximum at the cloud center and is reduced to half this value at a radius of about 1 mm. The maximum optical depth corresponds to a column density of 1.5×10^9 atoms/cm^2 using the value for the resonant absorption cross section of $\sigma_o = 1.39 \times 10^{-9}$ cm^2 [16].

The probe laser frequency was scanned across the resonance. Figure 4 shows the average laser absorption by the ultracold atom cloud as a function of frequency for the central ring and two outer rings. Data was taken by incrementing the laser frequency in steps as small as 0.5 MHz near resonance. This increment was increased to 6 MHz for frequencies further from resonance which were used
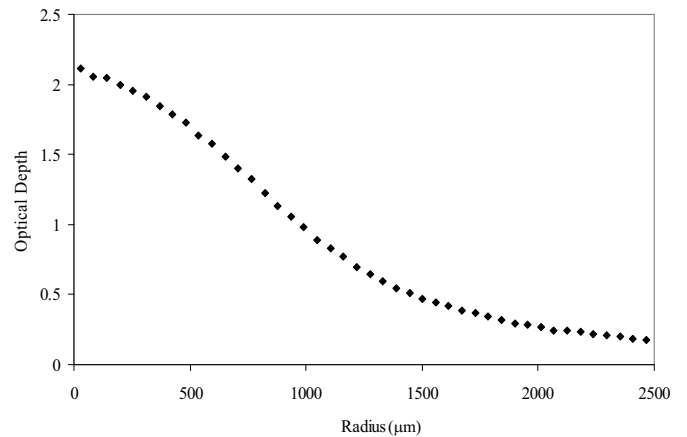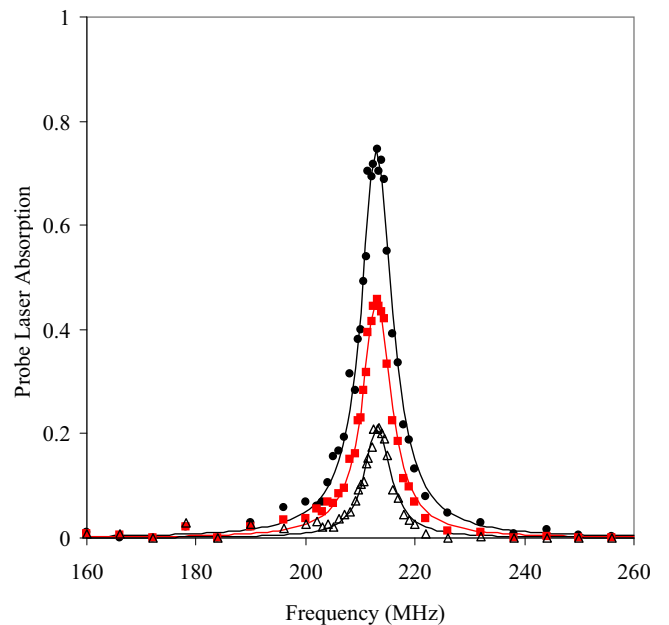
to determine the baseline. The data for each ring was well fit by a Lorentzian function using a minimization of least squares curve fitting algorithm. The fitted FWHM linewidth was next plotted versus the optical depth as shown in Figure 5. The linewidth at zero optical depth was determined for each run with a statistical uncertainty of ≤ 0.1 MHz by fitting a line to the data.

3 Results

A total of 57 data runs was taken on 17 days at several different laser powers using neutral density (ND) filters. Table 1 lists the average linewidths found at the different

Table 1. Observations of linewidth using different neutral density filters. The FWHM linewidth has been corrected for the laser intensity and has been extrapolated to zero optical depth as discussed in the text.

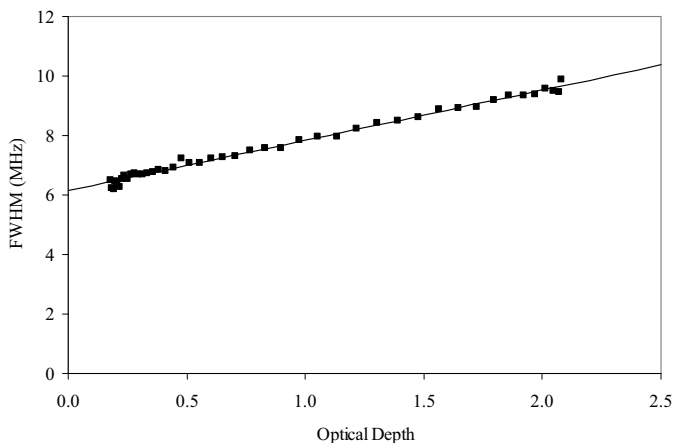| Average probe laser intensity (μW/cm^2)	FWHM linewidth at 0 OD (MHz)	Laser intensity correction (MHz)	Corrected FWHM linewidth (MHz)
41	6.173	−0.050	6.123 ± 0.021
115	6.343	−0.139	6.203 ± 0.024
150	6.339	−0.182	6.156 ± 0.034
		Average	6.158 ± 0.015

Fig. 5. Dependence of observed FWHM linewidth versus optical depth. The FWHM uncertainty of each point is comparable to the dot size. A line was fit to the data to extrapolate the linewidth at zero optical depth.

Table 2. Determination of natural linewidth.

Effect	Value (MHz)
Extrapolated linewidth at 0 O.D.	6.158 ± 0.015
Frequency jitter of probe laser	-0.091 ± 0.009
Residual Doppler broadening	−0.005
Zeeman broadening	<0.001
Collisions	<0.001
Lorentzian approximation of laser absorption lineshape	<0.001
Result for natural linewidth	6.062 ± 0.017

laser intensities. The maximum laser intensity was only about 5% of the saturation intensity 2.503 mW/cm^2 [17]. Hence, from equation (1), the natural linewidth at zero intensity γ_o, could be found by adding a correction

$$\Delta\gamma = -\frac{I}{2I_s}\gamma_o. \qquad (6)$$

Alternatively, one could compute the correction for each point in Figure 5. This was not done since the waist radius of the probe laser beam is four times larger than the 0.1 cm radius of the atom cloud. A 10% uncertainty in the average laser intensity experienced by the atoms encompassed the maximum intensity experienced by atoms at the cloud center and atoms at the cloud edge. The uncertainty of the final result in Table 1 incorporates the statistical uncertainty of the observed linewidths extrapolated to zero OD as well as the smaller uncertainty in laser intensity used to determine the correction given by (6).

Estimates of the contributions of other mechanisms that could affect the linewidth are given in Table 2. The largest broadening effect is due to frequency jitter of the probe laser which arises from the accuracy of the frequency lock circuit and the finite laser linewidth which is specified by the manufacturer to be less than 300 kHz over a 50 ms period. The laser frequency was locked using a saturation spectroscopic signal observed by passing the laser through a vapour cell as described earlier [13]. This signal contains a number of peaks separated by multiples/differences of the hyperfine splittings of the 5P$_{3/2}$ state. The latter have been determined with an uncertainty of only a few kHz and enable the frequency to be calibrated [18]. No assumption on the width of the hole burned lineshape, which is sensitive to various broadening effects, is required [19]. The intensity fluctuation of the frequency locked laser beam transmitted through the cell then provided an estimate of the frequency stability. The laser frequency was monitored for periods of time ranging from 0.1 ms to 1 s. The same result of 0.78 ± 0.05 MHz was found for the different time periods where the uncertainty was one standard deviation about the average.

The effect of the observed laser jitter on the linewidth listed in Table 2 was estimated by convoluting it with the absorption cross section given by (4). The resulting function closely matched the Lorentzian absorption cross section but had a slightly reduced amplitude which increased the FWHM linewidth by 0.091 ± 0.009 MHz. The uncertainty of this correction arises from the accuracy of the laser frequency stability.

Table 2 also lists the magnitudes of several possible broadening mechanisms. The residual Doppler broadening was estimated by calculating a Voigt profile and found to give a correction of 5 kHz. The correction arising from Zeeman broadening was estimated as follows. The linearly polarized probe laser pulse excited five transitions i.e. 5S$_{1/2}$ $F = 2\, m_F \rightarrow$ 5P$_{3/2}$ $F = 3\, m_F$ where the Zeeman sublevels are denoted by $m_F = 0$, ± 1, ± 2. The Zeeman shift of these transitions scales linearly with the field B and is given by $(g_F(5P_{3/2}) - g_F(5S_{1/2}))\, \mu_B B m_F$ where g_F is the g factor and μ_B is the Bohr magneton. The effect

Table 3. Lifetime of Rb $5P_{3/2}$ state.

Result (ns)	Technique
26.24 ± 0.04	Fast beam gas laser [6]
26.20 ± 0.09	Temporal fluorescence decay in MOT [7]
26.25 ± 0.08	Photoassociation spectroscopy [10]
26.26	Photoassociation spectroscopy [21]
26.25 ± 0.07	This work
26.42	Theory [11]
26.0	Theory [12]

on the lineshape was studied by summing the lineshapes for the transitions weighted using the appropriate Clebsch Gordon coefficients. The change of the FWHM of the lineshape for a 10 mG residual field is less than 1 kHz. The same result was found if the lineshape was generated by only considering laser excitation of atoms occupying the $5S_{1/2}$ $F = 2$ $m_F = \pm 2$ levels showing that optical pumping which could alter the relative populations of the m_F sublevels, had negligible effect on the linewidth.

The mean collision time between the ultracold atoms and residual gas in the vacuum chamber was estimated and found to be much greater than the probe laser pulse length. Similarly, collisions amongst the ultracold atoms were insignificant as the density of the cold atoms was several orders of magnitude lower than is the case for Bose Einstein condensates [14,20]. Effects such as radiation trapping and forward scattering which can be significant at higher densities were not evident. This was shown by the close agreement between the linear dependence of the observed linewidth on the optical depth as shown in Figure 5. The computed value of 1.68 MHz/OD agreed with the average observed slope of 1.59 ± 0.07 MHz/OD where the uncertainty is one standard deviation of the data about its average value.

Table 3 compares the lifetime computed from the natural linewidth using (2) with previous work. Volz and Schmoranzer [6] passed a fast rubidium ion beam through a gas cell. The resulting neutral atomic beam was intersected orthogonally by a cw dye laser beam. Fluorescence produced by the radiative decay of the $5P_{3/2}$ state was detected by a photomultiplier that was mounted on a translation stage. The signal was recorded as a function of the distance along the atomic beam. This experiment resolved discrepancies of the first excited state lifetimes of various alkali atoms obtained by different groups using the same technique, as well as differences with theory. The authors found that the fluorescent detection efficiency decreased slightly due to the divergence of the atomic beam. This led to an underestimate of the lifetimes by as much as 2%. They modeled the effect of beam divergence on fluorescence detection. This model was tested by measuring lifetimes of several transitions in neutral helium. Helium has a much lower mass than Rb resulting in a comparatively larger beam divergence. The He lifetimes corrected for the beam divergence effect agreed well with accurate ab initio theoretical calculations. This experiment reports a $5P_{3/2}$ lifetime accurate to better than 0.2% which requires

a very high signal to noise. Unfortunately, the paper does not present any data showing the temporal decay of the fluorescence used to derive this result.

Simsarian et al. [7] determined the lifetime by measuring the fluorescence of atoms excited in a MOT. The fluorescence was not found to be fit well by an exponential decaying function when the number of trapped atoms exceeded 1000. The authors speculate this may be due to radiation trapping or collisional quenching of the excited state. Lifetimes observed using a high number of trapped atoms differed from that obtained at a lower number of atoms by as much as 0.8% and were not included to determine the lifetime listed in Table 3.

Two groups [8,9] used photoassociation spectroscopy to study the formation of ultracold Rb_2 molecules. Photoassociation refers to the creation of a molecule that occurs when two atoms, each in the $5S_{1/2}$ ground state collide, and one of the atoms is excited by a laser to the $5P_{3/2}$ state. A molecule is formed if the resulting interaction has an attractive potential. These molecules can decay producing free atoms that are too energetic to remain in the trap. The interatomic potential depends on the matrix element between the $5S_{1/2}$ and $5P_{3/2}$ state that also determines the $5P_{3/2}$ radiative lifetime. Precise information is obtained by studying the rovibrational molecular states generated as a function of the photoassociation frequency.

Boesten et al. [8] studied ^{87}Rb atoms by focusing a 808 nm laser to create a 5 mK deep far off resonance optical dipole trap. The photoassociation laser had an intensity between 20 and 1000 W/cm^2. Gabbanini et al. [9] created cold rubidium molecules of both ^{85}Rb and ^{87}Rb isotopes at a temperature of ≈ 90 μK in a MOT. The photoassociation laser had a power of 70 mW and was focused to a spot smaller than the atom cloud in the MOT. Subsequent analysis of the data of these photoassociation experiments resulted in the lifetime estimates listed in Table 3 [10,21].

The $5P_{3/2}$ lifetime determined by this work agrees with that found using other experimental techniques. All of the experiments report lifetimes that are below the result of an ab initio relativistic many body theory calculation [11]. This difference is more than double the experimental uncertainty in every case. This theoretical value is also 1% higher than the result found using a hydrogenic potential to approximate the interaction of the alkali valence electron with the nucleus and inner electron cloud [12].

4 Conclusions

This work demonstrated a technique to directly measure the spectral linewidth of a transition. It is of interest for the study of line broadening that has primarily focused on systems where Doppler broadening remains significant [22]. The advantage of ultracold atoms is that Doppler broadening is negligible facilitating the study of other broadening effects such as due to collisions. The technique of monitoring the transmission of a laser through a cloud of atoms is also relatively simple. The spatial profile of the laser beam is readily observed by a

CCD camera which allows the study of the laser transmission as a function of the optical depth of the atom cloud. The detector can also be located a considerable distance from the atoms. This is important as trapping magnetic field coils frequently obscure the atom cloud making it difficult to place a photomultiplier close to the atoms to detect a significant fraction of the fluorescence.

The measurement of the natural linewidth allows the determination of the excited state lifetime. This allows an important test of experiments that determine lifetimes by observing the temporal decay of fluorescence which have in the past encountered subtle systematic effects at the level of a few percent that are not easily understood. The uncertainties can be especially significant for transitions having ultrashort lifetimes which have a correspondingly large natural linewidth. Hence, the technique of measuring the natural linewidth to determine the excited state lifetime may be especially useful for studying rapid transitions.

For the Rb $5P_{3/2}$ state, the lifetimes determined experimentally using three different techniques yield results with uncertainties of less than 0.3%. This is significant as the systematic effects that potentially influence these experiments are very different. These experimental results provide an important benchmark for theory. The measurement of linewidths therefore not only is of interest for studying broadening mechanisms but also is useful to test lifetimes determined using very different experimental techniques. These data in turn stringently test ab initio theory that takes into account relativistic and many body effects.

References

1. H.J. Metcalf, P. van der Straten, *Laser Cooling and Trapping* (Springer Verlag, New York, 1999)
2. C.W. Oates, K.R. Vogel, J.L. Hall, Phys. Rev. Lett. **76**, 2866 (1996)
3. W.A. van Wijngaarden, J. Li, *Spectral Line Shapes: AIP Conf. Proc.*, edited by A.D. May, J.R. Drummond, E. Oks, Toronto (1995), Vol. 8, pp. 252–253
4. W. Demtröder, *Laser Spectroscopy* (Springer Verlag, New York, 1988)
5. C. Guet, S.A. Blundell, W.R. Johnson, Phys. Lett. A **143**, 384 (1990)
6. U. Volz, H. Schmoranzer, Phys. Scripta T **65**, 48 (1996)
7. J.E. Simsarian, L.A. Orozco, G.D. Sprouse; W.Z. Zhao, Phys. Rev. A **57**, 2448 (1998)
8. H.M.J.M. Boesten, C.C. Tsai, J.R. Gardner, D.J. Heinzen, B.J. Verhaar, Phys. Rev. A **55**, 636 (1997)
9. C. Gabbanini, A. Fioretti, A. Lucchesini, S. Gozzini, M. Mazzoni, Phys. Rev. Lett. **84**, 2814 (2000)
10. R.F. Guetteres, C. Amiot, A. Fioretti, C. Gabbanini, M. Mazzoni, O. Dulieu, Phys. Rev. A **66**, 024502 (2002)
11. M.S. Safronova , W.R. Johnson, A. Derevianko, Phys. Rev. A **60**, 4476 (1999)
12. W.A. van Wijngaarden, J. Xia, J. Quant. Spectr. Rad. Trans. **61**, 557 (1999); W.A. van Wijngaarden, J. Quant. Spectr. Rad. Trans. **57**, 275 (1997)
13. B. Lu, W.A. van Wijngaarden, Can. J. Phys. **82**, 81 (2004)
14. H. Ming, W.A. van Wijngaarden, Can. J. Phys **85**, 247 (2007)
15. The CCD software did not have the ability to take a ratio of transmitted laser intensity with cold atoms present and absent such as shown in Figures 2a and 2b. The time to do this for each data point shown in Figure 4 is prohibitive and this signal ratio was therefore only done when the laser was in resonance to determine the dependence of the optical depth on the atom cloud radius as shown in Figure 3. The image of the atom cloud obtained taking the ratio I/I_o was virtually identical to that resulting from the CCD background subtraction
16. D.J. Han, PhD. Thesis, University of Texas, Austin, Texas, 1998
17. D.A. Steck, $^{87}Rb\ D\ Line\ Data$, Los Alamos National Laboratory, 2003
18. J. Ye, S. Swartz, P. Jungner, J.L. Hall, Opt. Lett. **21**, 1280 (1996)
19. S. Haroche, F. Hartmann, Phys. Rev. A **6**, 1280 (1972)
20. C. Fertig, K. Gibble, Phys. Rev. Lett. **85**, 1622 (2000)
21. This result was computed using data for the dispersion coefficient C$_3$ (in atomic units) given by $C_3\tau = 9/4\ \hbar\ (\lambda/2\pi)^3$ where τ is the excited state lifetime and λ is the transition wavelength as discussed in T. Bergeman, J. Qi, D. Wang, Y. Huang, H.K. Pechkis, E.E. Eyler, P.L. Gould, W.C. Stwalley, R.A. Cline, J.D. Miller, D.J. Heinzen, J. Phys. B, **39**, S813 (2006). This reference states no uncertainty limits for C$_3$ because of the high degree of correlation between the various fitted parameters. This result differs slightly from the lifetime of 26.23 ± 0.06 nsec listed in reference [7].
22. G. Peach, Collisional Broadening of Spectral Lines, in *Handbook of Atomic, Molecular & Optical Physics Part D* (Springer, New York, 2006), pp. 875-888